

## Homoclinic Tangle on the Edge of Shear Turbulence

Lennaert van Veen\*

*Faculty of Science, University of Ontario Institute of Technology, 2000 Simcoe Street North, Oshawa, L1H 7K4 Ontario, Canada*

Genta Kawahara†

*Graduate School of Engineering Science, Osaka University, 1-3 Machikaneyama, Toyonaka, Osaka 560-8531, Japan*

(Received 3 March 2011; published 8 September 2011)

Experiments and simulations lend mounting evidence for the edge state hypothesis on subcritical transition to turbulence, which asserts that simple states of fluid motion mediate between laminar and turbulent shear flow as their stable manifolds separate the two in state space. In this Letter we describe flows homoclinic to a time-periodic edge state that display the essential properties of turbulent bursting. During a burst, vortical structures and the associated energy dissipation are highly localized near the wall, in contrast with the familiar regeneration cycle.

DOI: 10.1103/PhysRevLett.107.114501

PACS numbers: 47.27.Cn, 47.27.ed, 47.52.+j

*Introduction.*—In recent years, the open problem of subcritical transition to turbulence in shear flows has seen a surge of interest, sparked by a rapidly increasing ability to perform numerical simulations as well as by a string of novel applications of dynamical systems theory. The dynamical systems approach advocates the idea that transitional shear flow is regulated by special solutions with a relatively simple spatial structure. They may be traveling waves, time-periodic solutions, or even solutions chaotic in time. Such states live in between a stable laminar state and stable, or metastable, turbulence. In simulations, these special states can be identified by a shooting algorithm in which initial data are iteratively refined to yield a flow which neither laminarizes nor becomes turbulent, but instead lingers on the “laminar-turbulent boundary” [1]. States on this boundary are necessarily unstable and consequently they can only be observed as transient effects in experiments [2]. Their relevance to the transition process lies mainly in their stable and unstable manifolds in state space. These determine how the fluid behaves as it transitions from near-laminar to turbulent states and vice versa.

A particularly interesting situation arises when the laminar-turbulent boundary is formed—at least locally—by the stable manifold of a traveling wave or periodic solution, which is then called an “edge state.” Edge states have now been computed for flow in channels as well as pipes, with various numerical schemes and resolutions, and there is some consensus that they are a robust feature of subcritical shear flow in the overlap of the dynamical systems and turbulence research communities [3].

Logically, the next step in this analysis would be to study the stable manifolds of the edge states. Knowledge of the geometry of these manifolds might open the door to the application of control techniques, aiming at a forced laminarization of the flow. Indeed, some results to this effect have been obtained using linearization about an edge state [4]. Little, if anything, is known about the global, nonlinear

structure of these separating manifolds, greatly reducing the usefulness and predictive power of the edge state hypothesis. The direct study of a separating manifold is hard if not impossible, owing to its high (formally infinite) dimensionality. In the current Letter, we study the two-dimensional unstable manifold of an edge state in plane Couette flow, using a novel computational algorithm, and find that it contains two orbits which return to the edge state along its stable manifold. We conjecture, that these homoclinic orbits collide and disappear in a tangency bifurcation at lower Reynolds number. Away from this bifurcation, these orbits generically are transversal intersections of the stable and unstable manifolds [5]. We conjecture that their presence thus implies the existence of an intricate tangle of these manifolds through the classical Smale-Birkhoff theorem [6]. This, in turn, may explain the observed chaotic dynamics of irregular turbulent bursting.

*Transitional plane Couette flow.*—We consider plane Couette flow at a Reynolds number of  $Re = 400$  in the minimal flow unit of dimensions  $L \times W \times H$ , where  $Re$  is based on half the velocity difference between the two walls  $U/2$  and half the wall separation  $H/2$ . The streamwise and spanwise periods are  $(L/H, W/H) = (2.76, 1.88)$  [7]. We used resolutions of  $16 \times 33 \times 16$  as well as  $32 \times 33 \times 32$  grid points in the streamwise ( $x$ ), wall-normal ( $y$ ), and spanwise ( $z$ ) directions, respectively, and checked that the behavior is qualitatively the same.

In this computational domain, the Nagata steady solution [8] does not exist [9]. Instead, the edge state in this flow is a time-periodic variation of the laminar flow, which shows weak, meandering streamwise streaks [4,10]. This gentle unstable periodic orbit (UPO) has a single unstable Floquet multiplier and thus its unstable manifold has dimension two and its stable manifold has codimension one in state space. Both the UPO and its unstable manifold are contained in a subspace invariant under the spatial

symmetries given by reflection in the midplane, followed by a streamwise shift over  $L/2$ , and reflection in the streamwise and spanwise direction, follow by a spanwise shift over  $W/2$ . Consequently, we can impose these symmetries on the solutions without placing artificial restrictions on the fluid motion. At the higher resolution, the number of degrees of freedom in the simulations is about 11 000.

*Homoclinic orbit computation.*—The unstable manifold of the UPO can be computed using multiple-shooting orbit continuation [11]. Essentially, this algorithm produces a sequence of orbits, contained in the manifold, by arclength continuation of a boundary value problem in time. Because of the extremely sensitive dependence on initial conditions in turbulent Navier-Stokes flow, we need to compose the orbits of multiple segments, each not much longer than the decorrelation time, i.e., the time scale of exponential divergence of turbulent states of fluid motion which are initially close. The results presented below use up to six segments, the integration time on each interval staying below 2 times the period  $T$  of the UPO and below 5 times the decorrelation time.

As we compute a sequence of orbits, it may happen that it converges to a homoclinic orbit, which separates the unstable manifold into two components. Two such orbits are shown in Fig. 1. In this projection on energy input and dissipation rate, the UPO is the tiny loop labeled  $L$ . In the background we have plotted the probability density function (PDF) of transient turbulence, computed from

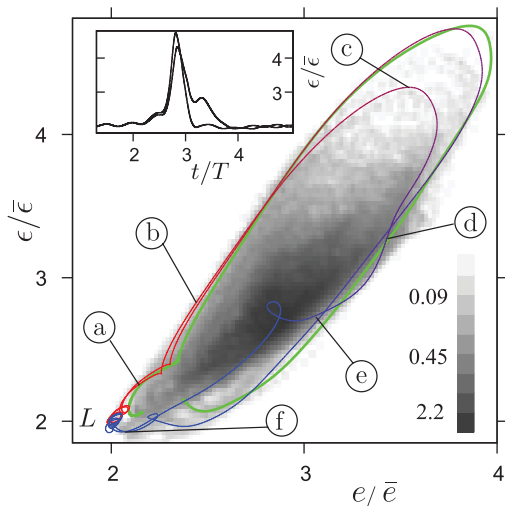


FIG. 1 (color). Projection of the homoclinic orbits onto energy input and dissipation rate, normalized by their value in laminar flow,  $\bar{e}$  and  $\bar{\epsilon}$ . The piece of orbit leaving the edge state  $L$  is shown in red and the one approaching it in blue. In the background, the PDF of transient turbulence is shown in gray scale. The labels (a)–(f) correspond to the snapshots in Fig. 2 and the green orbit segment is a spontaneous bursting event for comparison of the streamwise velocity profiles, see Fig. 4. The inset shows the dissipation rate of energy as a function of time along part of the homoclinic orbits.

direct numerical simulations starting from random initial conditions. In the transition to turbulence the homoclinic orbits overshoot the maximum of the PDF, then pass close to it on the way back to the UPO. They describe rare, extreme events, and the flow structure along them remains different from those associated with the regeneration cycle, as described below.

We generically expect homoclinic orbits to approach the UPO along its least stable subspace, also called the leading stable subspace. How well the depicted orbits approximate homoclinic connections can be quantified by measuring two distances: one from the end point of the computed orbits to the leading stable subspace at a point on the UPO and one to this point along the leading stable subspace. We found these distances to be of order  $10^{-6}$  and  $10^{-5}$ , respectively, in the energy measure, normalized by the mean energy along the UPO. To test the robustness of this result, we have recomputed the homoclinic orbits with a smaller integration time step and a varying number of shooting intervals.

*The flow structure of bursting.*—Figure 2 shows the time evolution of flow structures along the smaller homoclinic orbit at the six phases indicated in Fig. 1. The structures along the larger homoclinic orbit are qualitatively the same. In the early stage (phase *a*) the spanwise standing-wave motion of the streak is enhanced, so that the streamwise dependence, i.e., the three dimensionality, of the streak gradually becomes significant. At the same time the streak grows in the wall-normal direction. Such behavior is a consequence of the linear instability of the UPO, which has an eigenstructure characterized by disturbances of the streamwise velocity and vorticity highly localized on the crest and the valley of the streak.

As time progresses, the simultaneous spanwise oscillation and wall-normal growth of the streak exceed a critical level for bursting. There appear thin layers of extremely high vorticity between the wall and the crest and the valley of the streak, in which intense quasistreamwise vortex tubes are generated to induce high shear and thereby high energy dissipation (phase *b*). The quasistreamwise vortices of opposite signs of the streamwise vorticity align following the oscillation of the streak in the spanwise direction. Then the streak is rapidly deformed, while the second pair of quasistreamwise vortices appears on the crest and valley, and align with the first pair to form an array which moves fast on the crest or valley in the spanwise direction (phase *c*). During this streak deformation and vortex generation intense energy dissipation is observed in the thin layers between the wall and the crest or the valley of the streak. Streamwise vortices similar to those found in the regeneration cycle [7] and the corresponding strong UPO [10] also appear on the flanks of the streak. However, the streamwise vortices on the crest and valley of the streak are not observed in the near-wall regeneration cycle, and therefore we can say that these vortices are typical flow

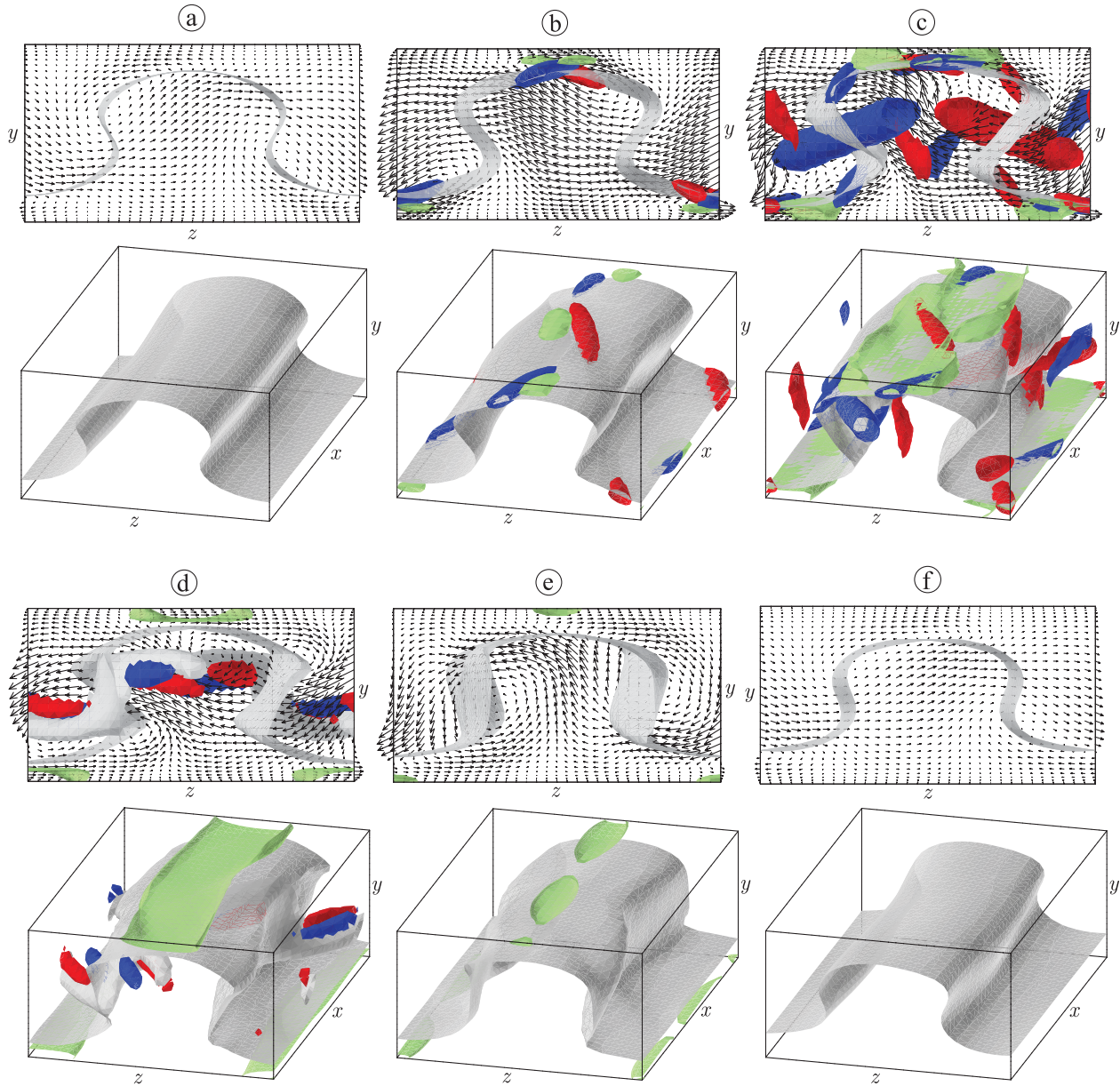


FIG. 2 (color). Visualization of flow structures in six phases on the smaller homoclinic orbit, labeled as in Fig. 1. Gray corrugated isosurfaces of the null streamwise velocity represent streamwise streaks. Isosurfaces at  $0.2(U/H)^2$  for the second invariant of a velocity gradient tensor are shown in red and blue and denote vortex tubes of clockwise and counterclockwise streamwise-vorticity component. Green isosurfaces show the local energy-dissipation rate at 20 times the value  $\bar{\epsilon}$  in laminar flow. In the midplane  $x = L/2$  the cross-stream velocity is shown, related to that at  $x = 0$  by a spanwise reflection under the flow symmetry.

structures of bursting with significant energy dissipation. Actually, an inspection of the turbulent state of plane Couette flow has shown that in bursting events of intense dissipation there appear similar vortex arrays on the crest and valley of the highly grown streak, which are associated with strong local dissipation. As shown in Fig. 3, the intense local dissipation (represented by green isosurfaces) observed around the crest and valley of the streak in Fig. 2 (phases *c* and *d*) contributes to the rapid increase of total energy dissipation (see Fig. 1). The identified high-dissipation regions occupy less than 10% of the spatial

domain but account for over 40% of the energy dissipation, implying that strong energy dissipation in the bursting event can be attributed to flow structures localized in the region around the crest and the valley of the streak shown by the green surfaces in Fig. 2. As time goes on, the highly deformed streaks are broken down (phase *d*), and then the streak and vortices decay rapidly (phase *e*) as the flow finally returns to a quiescent state close to the gentle UPO (phase *f*).

As reported by Kawahara and Kida [10], transient approaches of a turbulent state to relatively quiescent states

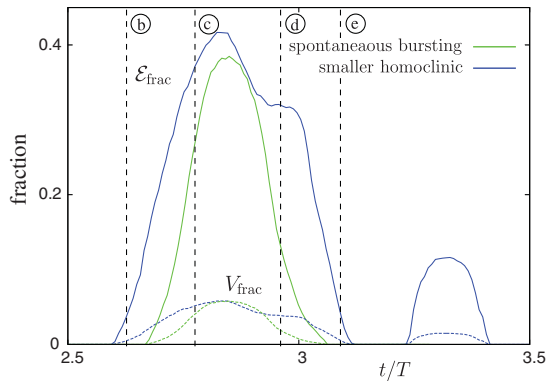


FIG. 3 (color). Blue: temporal variation of energy-dissipation (solid curve) and volume (dashed curve) fractions in the high-dissipation region bounded by the green surfaces in Fig. 2, with phases *b-e* as in that figure. Green: corresponding data for the spontaneous bursting segment.

of low energy input and dissipation are followed by bursting events with intense energy dissipation. The green curve in Fig. 1 is an example of such a spontaneous bursting event. In Fig. 4 we compare the streamwise velocity profile of this event to that of the homoclinic orbits and of turbulence, dominated by regeneration cycle dynamics. This comparison confirms that the physical processes of bursting are different from those of the regeneration cycle and that spontaneous bursting events tend to follow the homoclinic orbits in phase space.

Kawahara and Kida [10] suggested the interpretation of bursting in terms of a heteroclinic cycle between the gentle UPO and a UPO embedded in turbulent flow. The present analysis instead suggests that the process of the bursting may be related to homoclinic orbits.

*Conclusion.*—The existence of orbits homoclinic to the edge state implies that the geometry of the laminar-turbulent boundary is rather complex and we can expect to find a manageable approximation to it only locally. At the same time, it generically implies the existence of infinitely many UPOs which correspond to flows with arbitrarily many, arbitrarily long, near-laminarization events. It is natural then to think of turbulent shear flow as governed by a large chaotic attractor which comprises both UPOs in the turbulent regime, which reproduce the regeneration cycle [10], and UPOs which reproduce near-laminarization and bursting events. Physically, these bursting events are very different from the regeneration cycle. The streamwise vortices appear on the crest and valley of the streaks rather than on their flanks, and the larger part of the energy dissipation takes place in the near-wall, high strain region. The homoclinic solution presented here adds a new element to the elucidation of turbulence by means of dynamical systems theory, namely, that of temporal

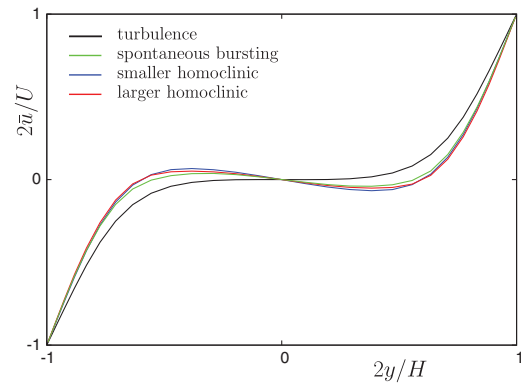


FIG. 4 (color). Comparison of streamwise velocity profiles, averaged over the streamwise and spanwise directions. The black line represents the turbulent time average. The bursting (green) and homoclinic (red, blue) profiles were averaged along the part of the orbit where  $\epsilon/\bar{\epsilon} > 4$ , i.e., around phase *c* in Fig. 2.

localization. Since it has been computed in a minimal flow unit, it cannot capture spatial intermittency. Recently, several equilibrium and traveling wave solutions exhibiting spatial localization have been found [12]. A clear goal for the near future is to find periodic or connecting orbits which combine the two forms of localization.

L. v. V. was supported by NSERC Grant No. 355849-2008. G. K. was supported by JSPS Grant-in-Aid for Scientific Research.

\*lennaert.vanveen@uoit.ca

†kawahara@me.es.osaka-u.ac.jp

- [1] T. Itano and S. Toh, *J. Phys. Soc. Jpn.* **70**, 703 (2001); *J. Fluid Mech.* **481**, 67 (2003).
- [2] Some evidence in pipe flow is discussed in T. Mullin, *Annu. Rev. Fluid Mech.* **43**, 1 (2011).
- [3] B. Eckhardt *et al.*, *Phil. Trans. R. Soc. A* **366**, 1297 (2008).
- [4] G. Kawahara, *Phys. Fluids* **17**, 041702 (2005).
- [5] See, e.g., Y.A. Kuznetsov, *Elements of Applied Bifurcation Theory* (Springer, New York, 2004), Chap. 7.2.1.
- [6] S. Smale, in *Differential and Combinatorial Topology* (Princeton University Press, Princeton, NJ, 1965), pp. 63–80.
- [7] J.M. Hamilton, J. Kim, and F. Waleffe, *J. Fluid Mech.* **287**, 317 (1995).
- [8] M. Nagata, *J. Fluid Mech.* **217**, 519 (1990).
- [9] J. Jiménez *et al.*, *Phys. Fluids* **17**, 015105 (2005).
- [10] G. Kawahara and S. Kida, *J. Fluid Mech.* **449**, 291 (2001).
- [11] L. van Veen, G. Kawahara, and A. Matsumura, *SIAM J. Sci. Comput.* **33**, 25 (2011).
- [12] T.M. Schneider, J.F. Gibson, and J. Burke, *Phys. Rev. Lett.* **104**, 104501 (2010); U. Ehrenstein, M. Nagata, and F. Rincon, *Phys. Fluids* **20**, 064103 (2008).